

## OBSERVATIONS OF INFLOW FEEDER CLOUDS AND THEIR RELATION TO SEVERE THUNDERSTORMS

*Rebecca J. Mazur<sup>1</sup>, John F. Weaver<sup>2,3</sup>, Thomas H. Vonder Haar<sup>2</sup>*

<sup>1</sup>*Department of Atmospheric Science, Colorado State University, Fort Collins, CO*

<sup>2</sup>*Cooperative Institute for Research in the Atmosphere, Colorado State University, Fort Collins, CO*

<sup>3</sup>*NOAA/NESDIS/RAMM Team, CIRA/CSU, Fort Collins, CO*

### 1. INTRODUCTION

Organized lines of cumulus towers within the inflow region of strong thunderstorms have been observed on satellite imagery (Weaver and Lindsey 2004; Weaver et al. 1994). These cumulus lines have been labeled inflow feeder clouds, or simply feeder clouds (Fig. 1). The relationship between feeder clouds and storm development and intensification has not been addressed extensively in the literature, nor has the occurrence of feeder clouds been objectively linked to severe weather<sup>1</sup>. However, understanding how feeder clouds relate to severe weather could have positive implications in severe storms forecasting and may add new insight into severe storm morphology. This study represents a first look at the relationship between their occurrence and severe weather.

Prediction of severe thunderstorms is complex since many interacting weather features both in the mesoscale and synoptic scales create an environment conducive to severe thunderstorm formation and intensification (Atkins et al. 1998; Klemp et al. 1981; Lemon and Doswell 1979; Purdom 1986; Weaver et al. 1994; Weaver and Purdom 1995; Weckwerth 2000; Weckwerth et al. 1996, Wilson et al. 1992). Meteorological observing systems such as surface and upper air observations do not resolve thunderstorms well since thunderstorms are considered sub-grid scale features on these observing networks. With satellite data, many observations of the atmosphere can be examined simultaneously to identify where a thunderstorm or group of thunderstorms will form, what factors will affect the evolution of the storm(s), what type of severe weather will occur (wind, hail, and/or

tornadoes), and how the storm(s) will propagate. In particular, storm scale cloud features on the order of 1-10 km are resolved on 1 km visible satellite imagery. These features (e.g. feeder clouds and flanking lines) have been studied using satellite imagery much less than other synoptic and mesoscale features, but often times are observed to be just as influential in storm evolution (Lemon 1976; Weaver and Lindsey 2004; Weaver and Purdom 1995; Weaver et al. 1994).

Another observing system that produces high resolution observations of thunderstorms is the Weather Surveillance Radar-88 Doppler (WSR-88D). Radar imagery taken from this system is heavily relied upon during warning operations to diagnose storm characteristics such as strength, size, and motion (Moller 2001). In particular, the Mesocyclone Detection Algorithm (hereafter MDA; Stumpf et al. 1998) is an automated radar algorithm that is used during severe weather situations to identify storms that have mesocyclones. Stumpf et al. (1998) found that 90% of storms in which mesocyclones were detected produced severe weather; therefore it is important to identify storms with mesocyclones during severe weather warning operations.

The MDA is currently run during real-time operations in all US National Weather Service Forecast Offices. It displays information about a mesocyclone's strength and size so that the forecaster can make an informed decision on whether the storm will produce severe weather. However, detecting tornadic and/or severe thunderstorms by identifying mesocyclones in radar data is very difficult to do with great skill. Thus it would be advantageous to develop supplementary methodologies to the MDA that could confirm questionable mesocyclones as well as provide information on the near storm environment to help assess the likelihood that such storms will strengthen and become severe. Satellite imagery is the ideal candidate for this role.

<sup>1</sup> Defined by the National Weather Service as hail > 0.75 in. in diameter, winds > 58mph (50kt), and/or tornadoes.

\* *Corresponding Author Address:* Rebecca J. Mazur, Dept. of Atmospheric Sciences, Colorado State University, Fort Collins, CO 80523. email: Mazur@cira.colostate.edu

Since the MDA is utilized during warning operations, it is suggested that adding information from visible satellite imagery (i.e. feeder cloud signatures) to the mesocyclone detection process might improve a forecaster's success in identifying and warning for severe storms. Although feeder clouds are not well understood in relation to thunderstorm development, Weaver and Lindsey (2004) suggest that feeder clouds may be a signal to rapid intensification in a storm and also may be an indication that a storm will soon produce severe weather. Therefore, this study will take a first look at whether a relationship does exist between the occurrence of feeder clouds and severe weather in a thunderstorm by establishing a time correlation between the two storm features. Also, feeder cloud signatures will be compared to mesocyclone detections from the MDA as predictors of severe weather. By establishing a correlation between feeder cloud signatures, mesocyclone detections, and severe weather, we hope to find some new insight into feeder cloud development and thunderstorm intensification as well as improve forecasting of severe weather.

## 2. DATA SOURCES

Feeder clouds can be observed using imagery from GOES Imager channel 1. Channel 1 collects radiation in the visible spectrum centered on  $.65\mu$  at 1 km. Images can be taken during normal scanning operations and rapid scan operations (RSO). RSO images are taken over the continental US at intervals that vary to include 5, 7, 10, and 12 minutes (Kidder and Vonder Haar 1995). Normal scanning operations take images every 15 minutes and a four-times daily full-disk scan that requires 30 minutes.

GOES-8 and 9 were the predecessors of the current GOES systems (10 and 12) and provided similar data as 10 and 12. For this study, visible imagery from all four satellites taken in RSO and normal scanning operations was examined for 24 days on which severe weather occurred. The purpose here is to observe how feeder clouds evolve in a storm and identify whether any relationship can be established between these cloud features and severe weather. RSO is useful during severe weather situations when environmental changes occur rapidly and animated loops can be used to highlight cloud features that are persistent over time (i.e. growing storms, overshooting tops,

cloud streets, etc.). A McIDAS<sup>2</sup> display system served as the visualization tool for displaying the imagery for this study.

Although visible imagery is useful in studying exterior storm scale features, the actual core of the storm cannot be observed by the GOES Imager. Observations of the storm core are available in three dimensions using the WSR-88D weather radar. In particular, the radial velocity product of the WSR-88D measures the averaged particle velocities in a beam volume toward and away from the radar and is used to detect areas of high wind and rotation in a storm (Burgess 1976; Moller 2001; Stumpf et al. 1998; Wood et al. 1996). Identifying rotation in a storm is important since storms with areas of strong cyclonic rotation, called mesocyclones, are likely to producing severe weather (Burgess 1976; Burgess et al. 1979; Jones et al. 2004; Lemon et al. 1977; Mitchell et al. 1998; and Stumpf et al. 1998).

The Mesocyclone Detection Algorithm (MDA) is an automated algorithm used in operational forecasting to identify circulations in storms that are mesocyclones. The MDA is used to assist the user in diagnosing which mesocyclones are more likely to represent a threat. Characteristics of the mesocyclone such as strength and size which may not be obvious to a human observer can be sampled using the MDA. Not all thunderstorms that produce severe weather have mesocyclones, but those storms with mesocyclones have a higher chance of producing hazardous weather and the MDA can be useful in identifying these storms.

For this study, MDA data for a subset of 9 of the 24 case study days were analyzed using CIRA's research AWIPS. Even though only a subset of radar data were analyzed compared to satellite data, if combining the two data systems will add any value to the severe weather prediction process, we should expect some indication of that fact using our case data.

## 3. FEEDER CLOUDS

Feeder clouds are small scale lines of cumulus towers that seem to occur most often in supercell thunderstorms. They are positioned ahead of the flanking line in the inflow region of a storm and are oriented roughly  $45^{\circ}$ - $135^{\circ}$  to the storm motion. Fig. 2 illustrates the proximity of

---

<sup>2</sup> The Man computer Interactive Data Access System (McIDAS) is a suite of applications for displaying and analyzing meteorological data.

feeder clouds to a thunderstorm's anvil and flanking line. Feeder clouds can be 5-50 km long and 5-10 km wide, and resemble horizontal convective rolls (HCR; having alternating clouds/no clouds co-located with regions of upward and downward motion, respectively). They are a steady feature relative to the storm, joining the "rain-free" updraft on its eastern edge (Weaver et al. 1994).

The mechanism(s) that initiate feeder clouds are unknown, but it seems that they form as a thunderstorm is rapidly intensifying. Oftentimes, feeder clouds will appear on visible imagery following an enhancement of the overshooting top (OST). An OST is a plume of cloud extending above the anvil (Fig. 2) that forms as the rapidly rising updraft air penetrates into the stratosphere above the anvil. An OST that is large in vertical and horizontal extent is indicative of a strong updraft (Rauber et al. 2002). Therefore, the appearance of feeder clouds concurrent with an enhancement of the OST on visible imagery suggests that feeder clouds may be forming as the updraft is strong and/or intensifying.

Feeder clouds also seem to appear on visible imagery as the flanking line becomes enhanced. Cumulus towers that make up the flanking line form on the leading edge of the rear flank downdraft (RFD; Fig. 2) and extend outward from the core of the storm (Bluestein 1993). Lemon (1976) showed that the flanking line is a source of storm intensification when cells from the line merge with the main updraft. The presence of the flanking line on visible imagery would therefore suggest that the storm is intensifying.

If feeder clouds occur during the development of these storm features, then it seems likely that feeder clouds could be forming as the storm is intensifying and may be in transition to become severe.

### **3.1 Observations of feeder clouds and mesocyclones in a supercell in Central Oklahoma on 8 May 2003**

This section will describe observations of a storm in which feeder clouds were observed. Storm features such as the OST, flanking lines, and mesocyclones will be discussed in relation to the occurrence of feeder clouds on satellite and radar imagery (Fig. 3). Storm reports will be used to indicate when the storm has become severe.

A supercell formed over central Oklahoma on the afternoon of 8 May 2003. The first towering cumulus clouds were observed

around 2015 UTC on a north-south oriented dryline. As the towers organized and moved eastward, the storm rapidly intensified, and storm splitting could be seen on radar beginning at 2116 UTC (not shown). By 2125 UTC, a large OST had formed and a mesocyclone was detected by the KTLX radar.

The 2132 UTC visible satellite image (Fig. 3a) shows a large OST with an anvil spreading from the updraft. This indicates that an intense updraft was developing although no mesocyclone was detected in the updraft region (Fig. 4d). The mesocyclone detected on the north flank was likely associated with the storm core north of the supercell, and so will not be discussed in this analysis. The supercell's inflow region is mostly indistinguishable on satellite imagery due to cirrus cloud cover therefore any fine scale structure (including developing feeder clouds) cannot be seen.

By 2145 UTC (Fig. 3b), the OST can be seen to have somewhat flattened out. Note also that the first feeder clouds have begun to show through the cirrus cover, coincident with a smaller, but persistent OST. At this time also, a well-defined flanking line had formed. Coincidentally, a mesocyclone was identified by the KTLX radar from 2136-2150 UTC (seen at 2145 UTC in Fig. 3e) and an inflow notch was persistent in the reflectivity field throughout this time period. The feeder clouds had grown in size and number by 2202 UTC (Fig. 3c) as the updraft reorganized to produce a single, well-defined overshooting top. On radar, reflectivity intensified to 55 dBZ and a hook echo had developed. The hook can be seen at 2200 UTC (Fig. 3f) coincident with a mesocyclone detection. This indicates rotation in the storm updraft was strong at this time. Following the enhancement of the feeder clouds on satellite and the hook echo in the reflectivity field on radar, large hail was reported in the storm at 2155 and 2158 UTC and an F0 tornado was reported at 2200 UTC.

The storm continued to increase in size both on satellite imagery and in radar reflectivity as it traveled ENE through Oklahoma. The hook appendage remained a persistent feature on radar imagery until 2235 UTC (not shown) and the feeder cloud deck continued to grow so that by 2210 UTC, they encompassed the entire inflow region. Mesocyclones were detected on radar from 2200 – 2225 UTC as the feeder cloud deck was growing and radar reflectivity values increased to 60dBZ by 2220 UTC. An F3 tornado was reported in this storm from 2210 -

2115 UTC and increased to F4 strength from 2115 – 2138 UTC. Unfortunately, soon after this time, the cirrus debris from a developing storm to the south began to mask the inflow region making it impossible to observe feeder clouds.

From this example, we see that feeder cloud development is associated with storm intensification and that severe weather can occur in a storm shortly after feeder clouds form. The overshooting top and flanking line became enhanced on satellite imagery and the reflectivity core seen on radar imagery intensified just prior to the formation of feeder clouds. Mesocyclone detections from the MDA were observed during this intensification phase as well. These observations support the notion that the formation of feeder clouds is a response to storm intensification. We were not, however, able to establish whether feeder clouds contribute to storm intensification.

## **4. SAMPLING AND TESTING METHODOLOGIES**

### **4.1 Thunderstorm Selection**

Since this study looks at the relationship between the occurrence of feeder clouds and severe weather, thunderstorms were chosen from days on which severe weather occurred. Days were chosen both in real time and from archived data. Older case days were picked based on recommendations by several severe weather research scientists and also by choosing randomly from the Storm Events database. The cases were chosen over various parts of the country during all seasons to keep the results more generalized.

Thunderstorms were selected using visible imagery prior to any analysis of storm reports. With no prior knowledge of storm severity, both severe and non-severe storms were sampled. It was important to include both storm types in order to diagnose whether feeder clouds are unique to severe thunderstorms. A storm was selected if the inflow region could be distinguished for a minimum of three RSO visible imagery scans (~15 min which allows time for storm scale features to evolve) or two images taken in normal scanning mode. It was further required that the selected storm was also quasi-steady state. Persistent storm features observed on satellite imagery (e.g. flanking line and OST) were used to make this determination. Based on these criteria, 131 storms were chosen from 24 severe weather days (Table 1).

### **4.2 Identifying Feeder Clouds, Mesocyclone Detections, and Severe Weather Reports in a Thunderstorm**

Once a storm was chosen, it was examined to see if feeder clouds, mesocyclones, and/or severe weather occurred. Each storm was first studied utilizing visible imagery alone from the first scan the inflow region was distinguishable until it could no longer be seen clearly. A storm was tracked using the OST as a reference point. The time of each scan analyzed, characteristics of the flanking line and OST (if present), and whether feeder clouds occurred were recorded for later statistical analysis.

A similar methodology was used for recording mesocyclones that occurred in a storm. Table 2 lists the cases used for the radar analysis. Each storm was identified on AWIPS radar output by associating the reflectivity core in time and space with its respective location on visible imagery using the lat/lon readout. The MDA output for each volume scan was then analyzed to determine which detections were mesocyclones. Similar to Trapp et al. (2005), detections were classified as mesocyclones if a circulation of strength rank-5 or greater was detected at or below 5 km above radar level, observed throughout a vertical depth  $\geq 3$  km, and persisted for a period longer than one radar volume scan (5 or 6 min) (for further details see Stumpf et al. (1998) and Trapp et al. (2005)). The mesocyclone detections that met these criteria were logged with visible imagery observations of a storm. If more than one detection in a storm met these criteria, then the strongest detection was used.

Once a storm was examined for feeder clouds and mesocyclones, storm reports were then associated with the storm to verify if it was severe in nature. Storm reports were taken from the NCDC Storm Events database and were compared in time and space using McIDAS. Each report was plotted on visible imagery using the city locator or lat/lon command on the scan that matched closest in time with the report. For a report to be associated with a storm, its location had to be in the storm core within 50 km of the parallax corrected OST. Occasionally, multiple storms occurred under an anvil even though only one OST was visible. Therefore, placing a distance constraint on the report relative to the parallax corrected OST was necessary to minimize the chance that a report was associated with a different storm core under the same anvil. Each report that matched with a

storm as identified on satellite and radar imagery was recorded for later statistical analysis.

#### 4.3 Scoring Methodology

For each storm report, a “time window” (Witt et al. 1998) encompassing the report was established as a means to classify and score each satellite and radar scan (and thus any features observed on those scans) as a predictor of severe weather. This classification and scoring procedures are a statistical method of quantitatively identifying a relationship between feeder cloud signatures and severe weather. The time window included any satellite or radar scan occurring up to 30 minutes prior to the beginning time of the severe weather event, and 10 minutes after the ending time of the event. The 30 minute time period allowed for at least two visible imagery scans to be examined with sufficient lead time to predict the event. The 10 minute time period after the event was necessary to account for errors in the storm reports. If the storm report happened to fall at the end of a thirty minute gap in visible imagery, the report was not used for scoring purposes since feeder clouds can evolve on time scales much less than 30 minutes.

Table 3 is a contingency table used to classify each of these predictions. If feeder clouds were observed in a storm, each scan on which they were visible was considered a positive, or “yes” algorithm prediction of severe weather. All scans that feeder clouds were not visible were considered a negative, or “no” algorithm prediction. An observed event is defined as a scan that falls within the time window of a severe weather report (“yes” event) or a scan that occurs outside the time window (“no” event).

Each “yes” algorithm prediction during the time window was considered a *hit* (classified as contingency “a”). Each “no” algorithm prediction within the time window was considered a *miss* (contingency “c”). If no severe weather was reported but feeder clouds were observed, or if feeder clouds were observed in a storm outside the time window of a severe weather report, then each scan was considered a *false alarm* (FA; contingency “b”). If no severe weather was reported, and no feeder clouds were observed in a storm, then each scan was considered a *correct no prediction* (CNP; contingency “d”).

The same classification scheme was used to evaluate mesocyclone detections as well as for the combined detections by feeder cloud signatures and mesocyclone detections.

Combined detections are defined in this study as a satellite imagery scan that occurs at the same time or within three minutes of a radar imagery scan. Additional combined detections are tallied for each satellite and radar scan that occurs more than 3 minutes apart from another. An example of how each satellite and radar scan is classified is illustrated in Table 4. The portion highlighted in blue includes the scans that fall within the (-30, +10) time window.

Each category from Table 3 was then tallied and the probability of detection (POD), false alarm rate (FAR), and critical success index (CSI) were calculated using the following relationships:

$$\text{POD} = a / (a + c) \quad (1)$$

$$\text{FAR} = b / (a + b) \quad (2)$$

$$\text{CSI} = a / (a + b + c) \quad (3)$$

The POD, FAR, and CSI are skill scores used to quantitatively identify any relationship between the occurrence of feeder clouds and severe weather as well as to evaluate each storm feature as a potential predictor of severe weather separately, and together to see which has the most predictive skill.

## 5. RESULTS

The classification of predictions for feeder cloud signatures are summarized in Fig. 4. From the 131 storms chosen for this study, a total of 1238 visible imagery scans were classified using Table 3. The classification yielded 269 hits (21.7% of all visible imagery scans), 81 false alarms (FA; 6.5%), 497 misses (40.1%), and 391 correct “no” predictions (CNP; 31.6%). From these results, we see that a considerable number of severe weather events were not predicted by feeder cloud signatures since 40.1% of all visible imagery scans were classified as missed predictions and 21.7% were hits. Therefore, it is clear that feeder clouds are not a necessary condition for severe weather to occur in a storm. Combining the misses and CNP categories, we see that 71.7% of all storms did not produce feeder clouds. This implies that in general, feeder clouds may not be a commonly seen feature in thunderstorms.

As seen in Fig. 5, feeder cloud signatures score relatively low in overall prediction of severe weather (POD = 35.1% and CSI = 31.8%). Clearly, feeder cloud signatures are not very good at predicting all severe weather. However, the low FAR (23%) suggests that if feeder clouds are observed in a storm, there is a good chance (77%) that severe weather will occur within 30 min of that

observation. In those cases, the storm has a high probability of producing severe weather shortly after the occurrence of feeder clouds. This result supports the notion that feeder clouds may be associated with intensification in some storms since they often form as the storm transitions from non-severe to severe.

The classification of predictions by the MDA is summarized in Fig. 6. From the subset of 9 cases, 46 storms were examined for mesocyclone detections and 899 radar volume scans were classified using the criteria described in section four. The classification yielded 322 hits (35.8% of all radar scans), 46 false alarms (5.1%), 356 misses (39.6%), and 175 CNP (19.5%). Again, there were a high percentage of misses (39.6%) indicating that the majority of severe weather that occurred was not predicted by the MDA. Similar to feeder cloud signatures, it is suggested that mesocyclones are not necessary for a storm to produce severe weather. Combining misses with CNP we see that 59.1% of all radar scans did not have mesocyclones, implying that mesocyclones are not common to all storms in the study.

Fig. 7 summarizes the skill scores for predictions by the MDA. The MDA outperforms feeder cloud signatures since the POD (47.5%) and CSI (44.5%) are higher. The FAR (12.5%) is lower, suggesting that if a mesocyclone is detected in a storm, there is a higher likelihood (87.5%) compared to feeder clouds (77%) that severe weather will occur within 30 min. These results suggest that the MDA has skill in predicting severe weather.

The 9 cases (46 storms) analyzed using radar imagery were combined with the results for the same 9 cases from the satellite analysis to classify and score combined detections. A total of 906 combined visible imagery and radar comparisons were classified, and the results are summarized in Fig. 8. The classification yielded 402 hits (44.4% of combined detections), 71 FA (7.8%), 285 misses (31.5%), and 148 CNP (16.3%). For this classification, 52.2% of combined detections saw mesocyclone detections and/or feeder cloud signatures meaning that these features were observed in over half the storms examined in this section. The percentage of hits (44.4%) is higher than the percentage of misses (31.5%), meaning that the combined detections have diagnosed more severe weather events than either the occurrence of feeder clouds or mesocyclone detections did alone. These preliminary results based on a small data set are

encouraging; however, a 44.4% hit ratio means that numerous severe weather events were still not predicted. This result further supports the notion that a storm can produce severe weather without the presence of feeder clouds or mesocyclones.

On the whole, combined detections outperformed both feeder cloud signatures and mesocyclone detections as sole predictors of severe weather. As seen in Fig. 9, the POD (58.5%) and CSI (53%) have improved by 10-20% meaning that the combination of feeder cloud signatures and mesocyclone detections has more skill in predicting all types of severe weather than as separate predictors. The low FAR (15%) indicates that when feeder clouds, mesocyclone detections, or both storm features are observed on satellite and/or radar, there is an 85% likelihood that severe weather will occur within 30 min. The FAR for the combined detections is 2.5% worse than that for MDA detections alone, and 7% better than that calculated for feeder cloud signatures. However, all three methods have reasonably low FAR's.

For further confirmation, a simple two-sample hypothesis test was run on the MDA results alone versus the combined MDA and feeder cloud results. The test showed that there is sufficient evidence to conclude that both the POD and CSI for the combined data set is significantly higher than those for the MDA alone, at a 1% level of significance. Since the MDA is currently utilized during warning operations as a predictor of severe weather, it is suggested that adding feeder cloud signatures to warning operations may be a useful adjunct to the MDA when diagnosing a storm's potential to produce severe weather.

Fig. 10 is a summary of the skill scores for feeder cloud signatures, MDA detections, and combined detections. The results from this analysis indicate that combined detections are the most skilled predictors of severe weather in terms of POD and CSI. In terms of FAR, MDA seems best, but considering the limited size of the radar dataset, perhaps not significantly so. The FAR for the combined detections may be worse than the MDA (by 2.5%), but the POD and CSI are 10-20% higher than both feeder cloud signatures and MDA detections. Therefore, by using feeder cloud signatures in combination with mesocyclone detections from the MDA, the likelihood that severe weather will be accurately predicted with some lead time is

better than by using either storm feature as separate predictors.

## **6. CONCLUSIONS AND SUGGESTIONS FOR FUTURE WORK**

### **6.1 Conclusions**

Based on observations taken of feeder clouds, mesocyclone detections from the Mesocyclone Detection Algorithm (Stumpf et al. 1998) and severe weather reports in a storm, this study has established a relationship between the occurrence of feeder clouds and severe thunderstorms. We have shown:

a) Combining the qualitative analysis of the occurrence of feeder clouds in severe thunderstorms (described in section three) with the quantitative results described section five supports the hypothesis that feeder clouds are an indication that a storm is rapidly intensifying and may produce severe weather soon thereafter. Feeder clouds are not necessary for severe weather to occur, but there is evidence to put forward the idea that they are a response to the intensification of some non-severe storms as they transition to become severe storms. Since storms with feeder clouds are more likely (77%) to produce severe weather within 30 minutes, it is suggested that there is a likely relationship between the two storm features.

b) Adding feeder cloud signatures to the MDA during severe weather operations will improve forecasters' skill in warning for severe weather. By correlating the occurrence of feeder clouds with severe weather reports, this study found that feeder cloud signatures have low skill in predicting severe weather (POD = 35.1% and CSI = 31.8%) but the FAR (23%) suggests that if feeder clouds are observed in a storm, there is a 77% chance that severe weather will occur within 30 min. Feeder clouds were observed in only 28.3% of the storms analyzed for this study, therefore they may not be common to all thunderstorms. The low POD and CSI imply that feeder clouds are not necessary for severe weather to occur, but the high probability that severe weather will occur when they are observed suggests that they have predictive value.

In comparison to the skill of the MDA at predicting severe weather (POD = 47.5%, CSI = 44.5%, and FAR = 12.5%), feeder cloud signatures were outperformed in all three categories. Furthermore, combined detections outperformed both feeder cloud signatures and mesocyclone detections as sole predictors of severe weather. The POD (58.5%) and CSI

(53%) for combined detections represents a 10-20% improvement, meaning that the combination of feeder cloud signatures and mesocyclone detections has more skill in predicting all types of severe weather than each have as separate predictors. The low FAR (15%) indicates that when feeder clouds, mesocyclone detections, and/or both storm features are observed on satellite and/or radar, there is an 85% likelihood that severe weather will occur within 30 min. Therefore, a quick check for feeder cloud signatures on visible satellite imagery would seem to be a useful adjunct to radar imagery in the warning decision making cycle.

### **6.2 Suggestions for Future Work**

It would be interesting to obtain radar data for all 24 cases in order to provide a more comprehensive comparison between the satellite and radar imagery used in this study. It might also be beneficial to expand the current satellite database (and subsequently the radar database) to include more storms in mountainous and coastal regions which were not well represented in this study.

Recalculating the POD, FAR, and CSI for the feeder cloud signatures according to severe weather type and strength may provide information on what type of severe weather occurs most often in storms with feeder clouds and whether feeder cloud signatures are better at predicting a certain type/strength of severe weather.

It may also be beneficial to try time windows of different lengths in order to obtain a more comprehensive evaluation (Witt et al. 1998) since the time window used in this study was a first guess at identifying a time correlation between the formation of feeder clouds and severe weather.

Field research efforts could be used to diagnose the state of the atmosphere during times when feeder clouds are present or developing to discover how/why feeder clouds form. In-situ observations would help increase our understanding of feeder cloud evolution in a thunderstorm from a ground-based perspective.

Lastly, if high resolution numerical models are able to reproduce feeder clouds, the output might be useful in diagnosing the mechanisms that lead to their formation in relation to storm intensification. By simulating supercells with initial conditions that are conducive to feeder cloud development, we might be able to discover whether feeder clouds are solely a response to rapid intensification of a

storm, or if their underlying structure similar to that of HCR's somehow contributes to storm intensification. Field observations, combined with high resolution model analysis, seem the next logical step toward understanding these storm features.

## 7. REFERENCES

Atkins, N. T., R. M. Wakimoto, and C. L. Ziegler, 1998: Observations of Finescale Structure of a dryline during VORTEX 95. *Mon. Wea. Rev.*, 126, 525-550.

Bluestein, H. B., 1993: *Synoptic-Dynamic Meteorology in Midlatitudes*. Oxford University Press, 594 pp.

Burgess, D. W., 1976: Single-Doppler radar vortex recognition. Part I: Mesoscale signatures. Preprints, 17th Conf. on Radar Meteorology, Seattle, WA, Amer. Meteor. Soc., 97-103.

\_\_\_\_\_, R. J. Donaldson, T. Sieland, and J. Hinkelman, 1979: Final Report on the Joint Doppler Operational Project (JDOP 1976-1978). Part I: Meteorological Applications. NOAA Tech. Memo. ERL NSSL-86, NOAA, Boulder, CO, 84 pp. [NTIS PB80-107/88/AS.]

Jones, I. A., K. M. McGrath, and J. T. Snow, 2004: Association between NSSL Mesocyclone Detection Algorithm-Detected vortices and tornadoes. *Wea. Forecasting*, 19, 872-890.

Kidder, S. Q. and T. H. Vonder Haar, 1995: *Satellite Meteorology: An Introduction*. Academic Press, 466 pp.

Klemp, J. B., R. B. Wilhelmson, and P. S. Ray, 1981: Observed and numerically simulated structure of a mature supercell thunderstorm. *J. Atmos. Sci.*, 38, 1558-1580.

Lemon, L. R., 1976: The flanking line, a severe thunderstorm intensification source. *J. Atmos. Sci.*, 33, 686-694.

\_\_\_\_\_, R. J. Donaldson, Jr., D. W. Burgess, and R. A. Brown, 1977: Doppler radar application to severe thunderstorm study and potential real-time warning. *Bull. Amer. Meteor. Soc.*, 58, 1187-1193.

\_\_\_\_\_ and C. A. Doswell, III, 1979: Severe thunderstorm evolution and mesocyclone

structure as related to tornadogenesis. *Mon. Wea. Rev.*, 107, 1184-1197.

Mitchell, E. D., S. V. Vasiloff, G. J. Stumpf, A. Witt, M. D. Eilts, J. T. Johnson, and K. W. Thomas, 1998: The National Severe Storms Laboratory Tornado Detection Algorithm. *Wea. Forecasting*, 13, 352-366.

\_\_\_\_\_, 2001: Severe local storms forecasting. *Severe Convective Storms, Meteor. Monogr.*, No. 50 Amer. Meteor. Soc., 433-480.

\_\_\_\_\_, 1986: Convective scale interaction: Arc cloud lines and the development and evolution of deep convection. Ph.D. thesis, Dept of Atmospheric Science, Colorado State University, 197 pp.

Rauber, R. M., J. E. Walsh, and D. J. Charlevoix, 2002: *Severe and Hazardous Weather*. Kendall/Hunt Publishing Company, 616 pp.

Stumpf, G. J., A. W. Witt, E. D. Mitchell, P. L. Spencer, J. T. Johnson, M. D. Eilts, K. W. Thomas, and D. W. Burgess, 1998: The National Severe Storms Laboratory Mesocyclone Detection Algorithm for the WSR-88D. *Wea. Forecasting*, 13, 304-326.

Trapp, R. J., G. J. Stumpf, and K. L. Manross, 2005: A reassessment of the percentage of tornadic mesocyclones. *Wea. Forecasting*, 20, 680-687.

\_\_\_\_\_, J. F. W. Purdom, and K. J. Szoke, 1994: Some mesoscale aspects of the 6 June 1990 Limon, Colorado, tornado case. *Wea. Forecasting*, 9, 45-61.

\_\_\_\_\_ and \_\_\_\_\_, 1995: An interesting mesoscale storm-environment interaction observed just prior to changes in severe storm behavior. *Wea. Forecasting*, 10, 449-453.

\_\_\_\_\_ and D. Lindsey, 2004: Some frequently overlooked severe thunderstorm characteristics observed on GOES imagery: A topic for future research. *Mon. Wea. Rev.*, 132, 1529-1533.

Weckwerth, T. M., J. W. Wilson, and R. M. Wakimoto, 1996: Thermodynamic variability within the convective boundary layer due to

horizontal convective rolls. *Mon. Wea. Rev.*, 124, 769-784.

\_\_\_\_\_, 2000: The effect of small-scale moisture variability on thunderstorm initiation. *Mon. Wea. Rev.*, 128, 4017-4030.

Wilson, J. W., G. B. Foote, N. A. Crook, J. C. Fankhauser, C. G. Wade, J. D. Tuttle and C. K. Mueller, 1992: The role of boundary-layer convergence zones and horizontal convective rolls in the initiation of thunderstorms: A case study. *Mon. Wea. Rev.*, 120, 1785-1815.

Witt, A., M. D. Eilts, G. J. Stumpf, E. D. Mitchell, J. T. Johnson, and K. W. Thomas, 1998: Evaluating the performance of WSR-88D severe storm detection algorithms. *Wea. Forecasting*, 13, 513-518.

Wood, V. T., R. A. Brown, and D. W. Burgess, 1996: Duration and movement of mesocyclones associated with southern Great Plains thunderstorms. *Mon. Wea. Rev.*, 124, 97-101.

8. FIGURES AND TABLES

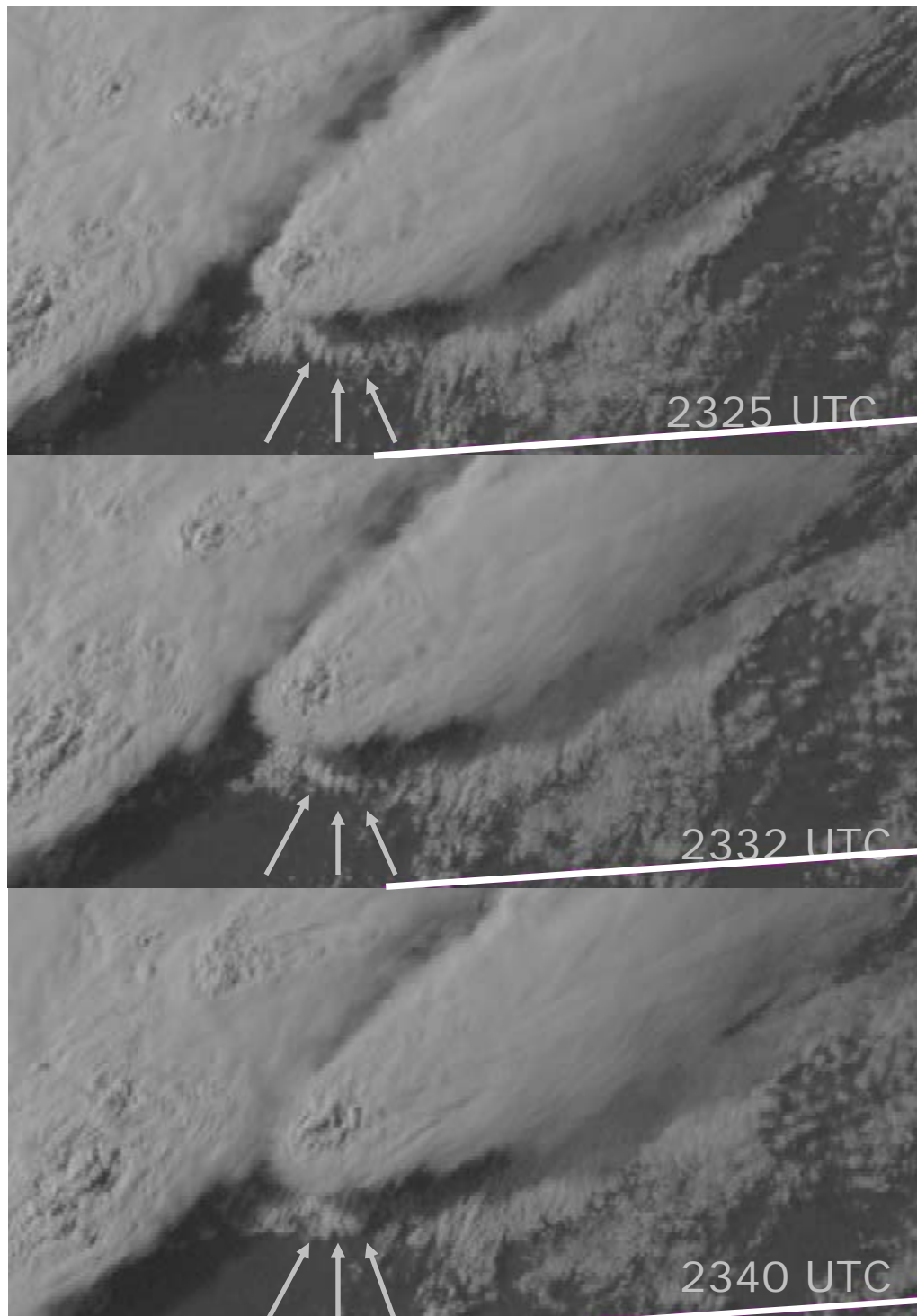


Fig. 1. Visible satellite imagery taken on 7 June 2005 at 2325 UTC, 2332 UTC, and 2340 UTC over SE South Dakota. Arrows denote the location of feeder clouds.

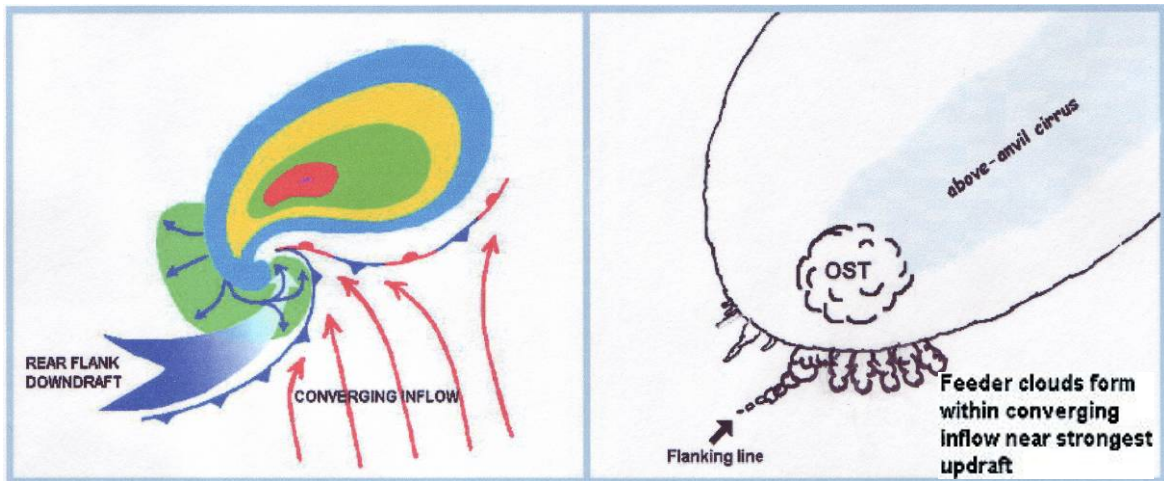


Fig. 2. Schematic diagram of a supercell thunderstorm showing a plan view of (left) an idealized, base-reflectivity radar echo, the RFD and gust front (depicted by the cold front symbol) and (right) a satellite representation of the same storm showing feeder clouds in relation to the flanking line and anvil of a supercell thunderstorm. Adapted from Weaver and Lindsey, (2004).

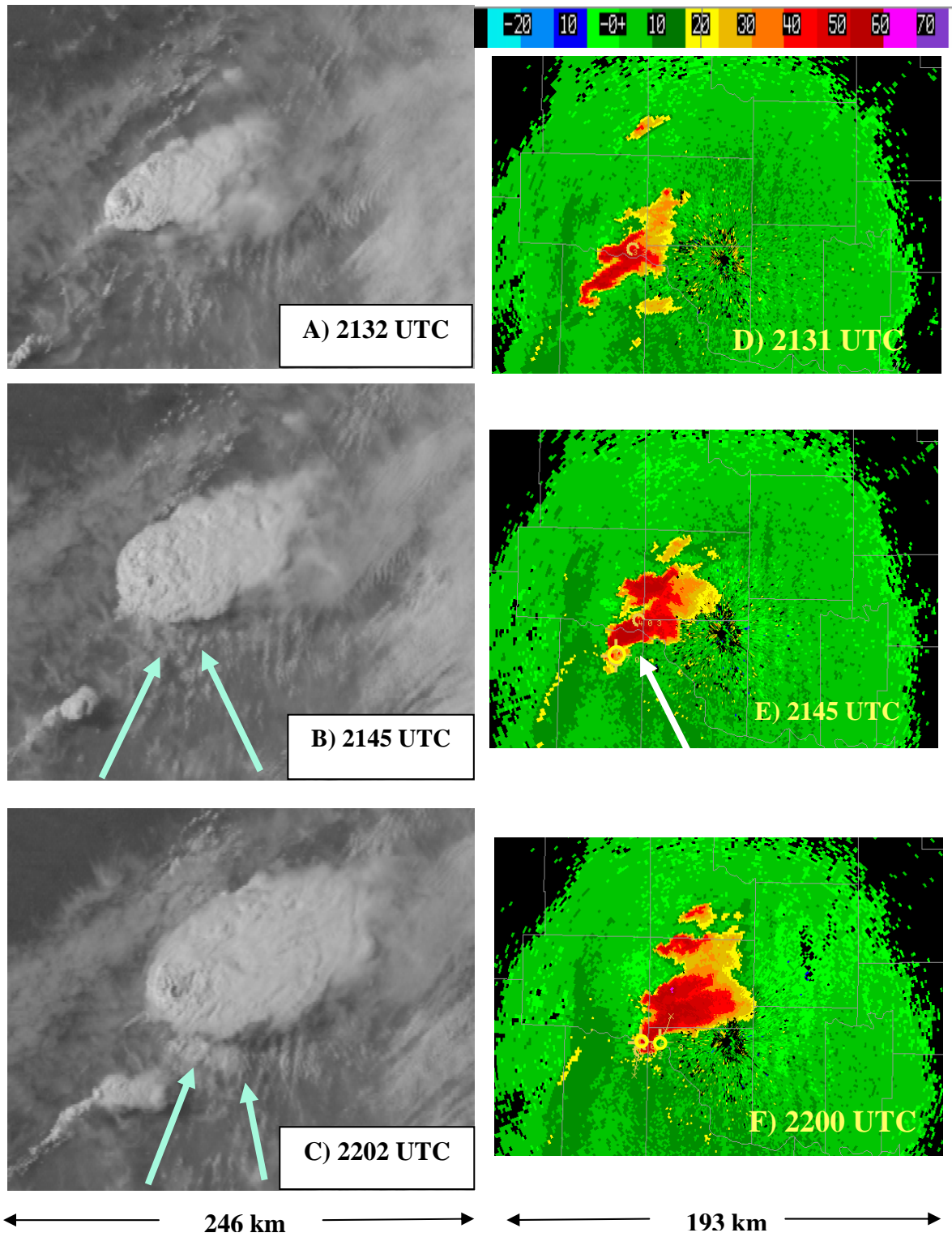


Fig. 3. GOES-12 1 km visible images (left) and base reflectivity from KTLX (right) of the supercell in central Oklahoma 8 May 2003. Feeder clouds are denoted by the cyan arrows and mesocyclone detections are denoted as the yellow circles. The white arrow denotes the region of the inflow notch.

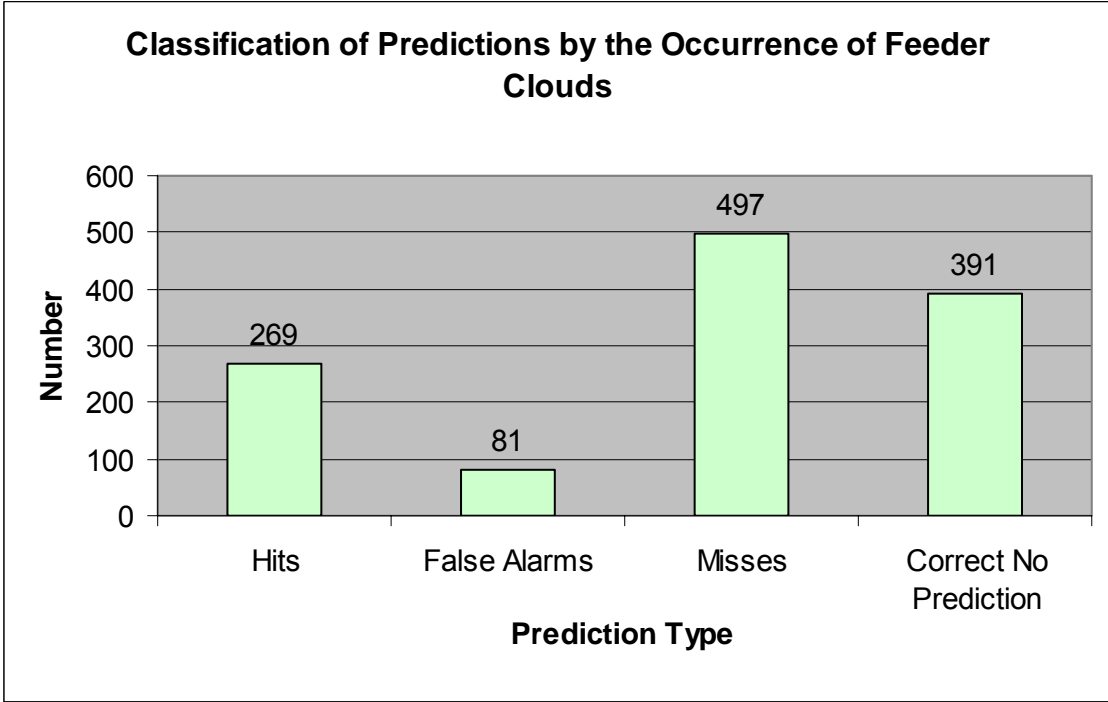


Fig. 4. Summary for severe weather predictions utilizing the occurrence of feeder clouds as a sole predictor.

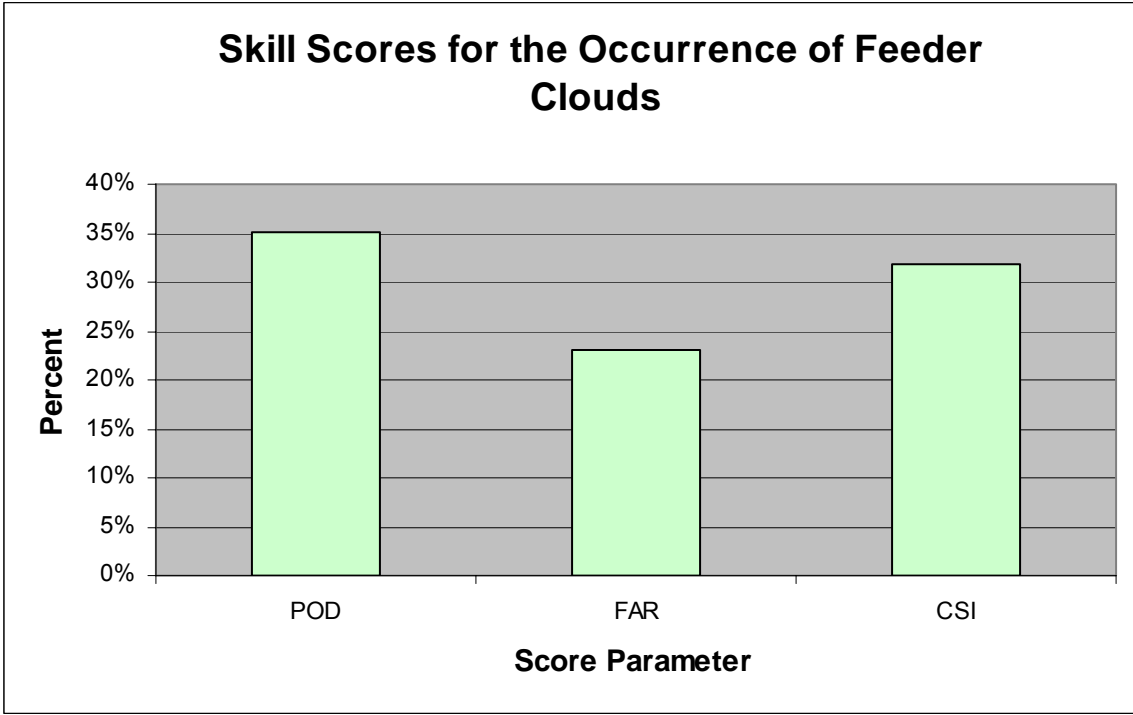


Fig. 5. Skill scores for the utilization of feeder clouds as sole predictors of severe weather. POD, FAR, and CSI are defined by Eqs. (1-3), respectively.

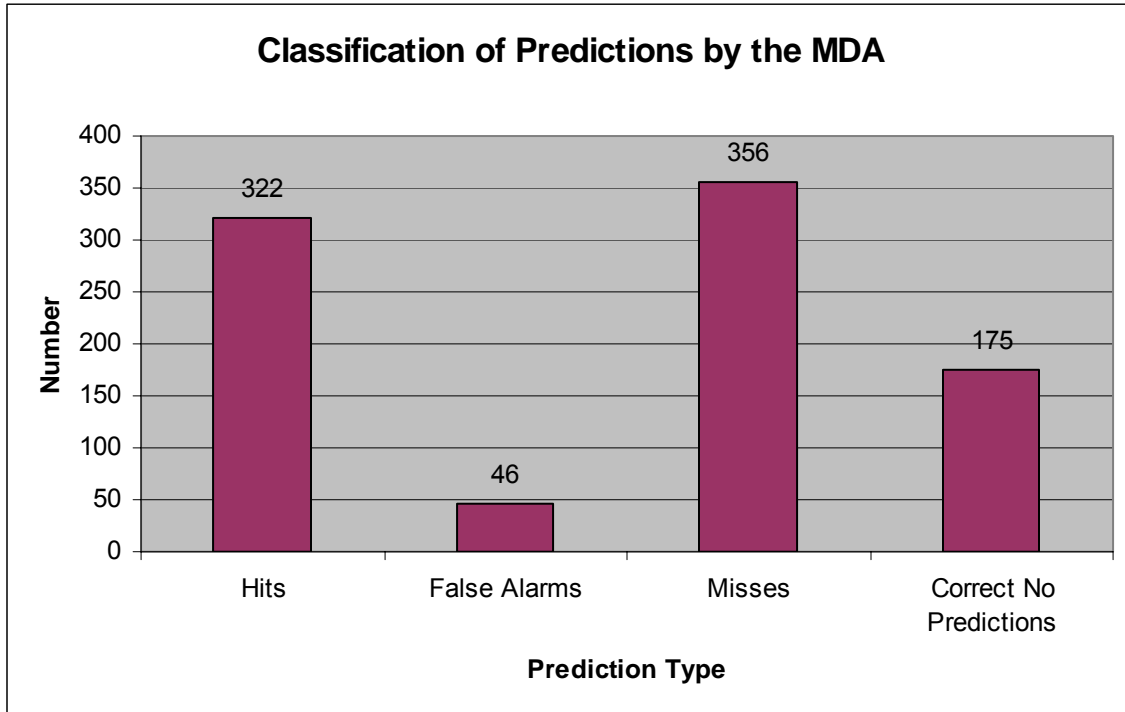


Fig. 6. Summary for severe weather predictions utilizing mesocyclone detections from the MDA as sole predictors.

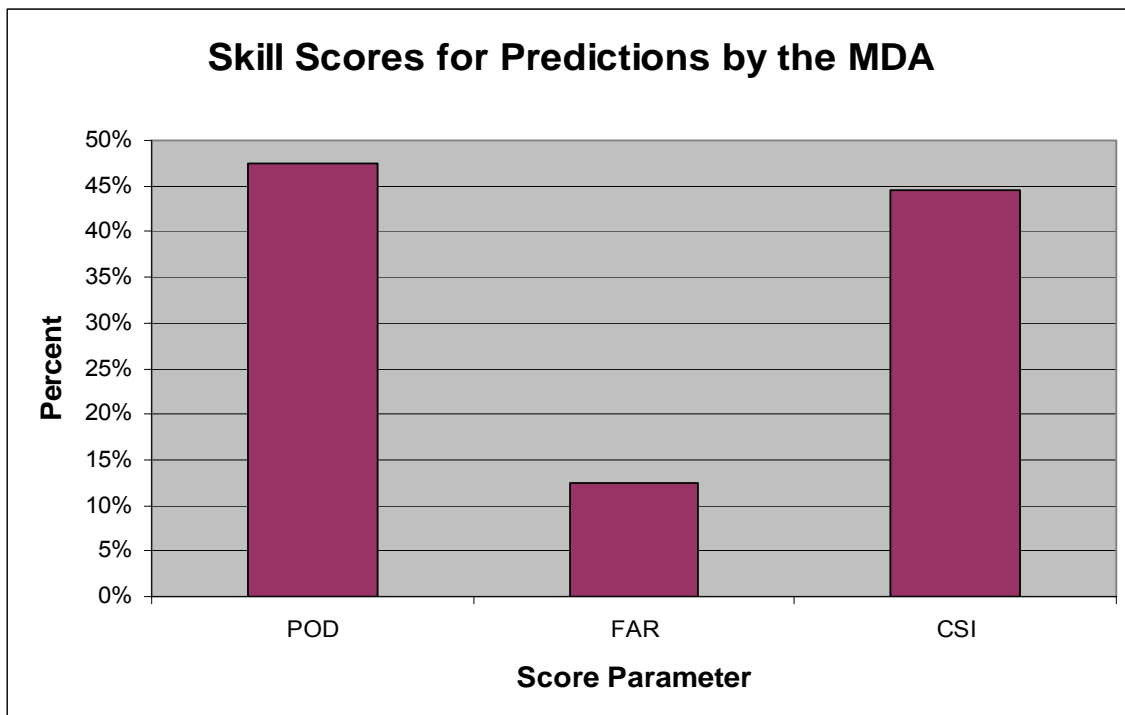


Fig. 7. Skill scores for the utilization of mesocyclone detections from the MDA as sole predictors of severe weather. POD, FAR, and CSI are defined by Eqs. (1-3), respectively.

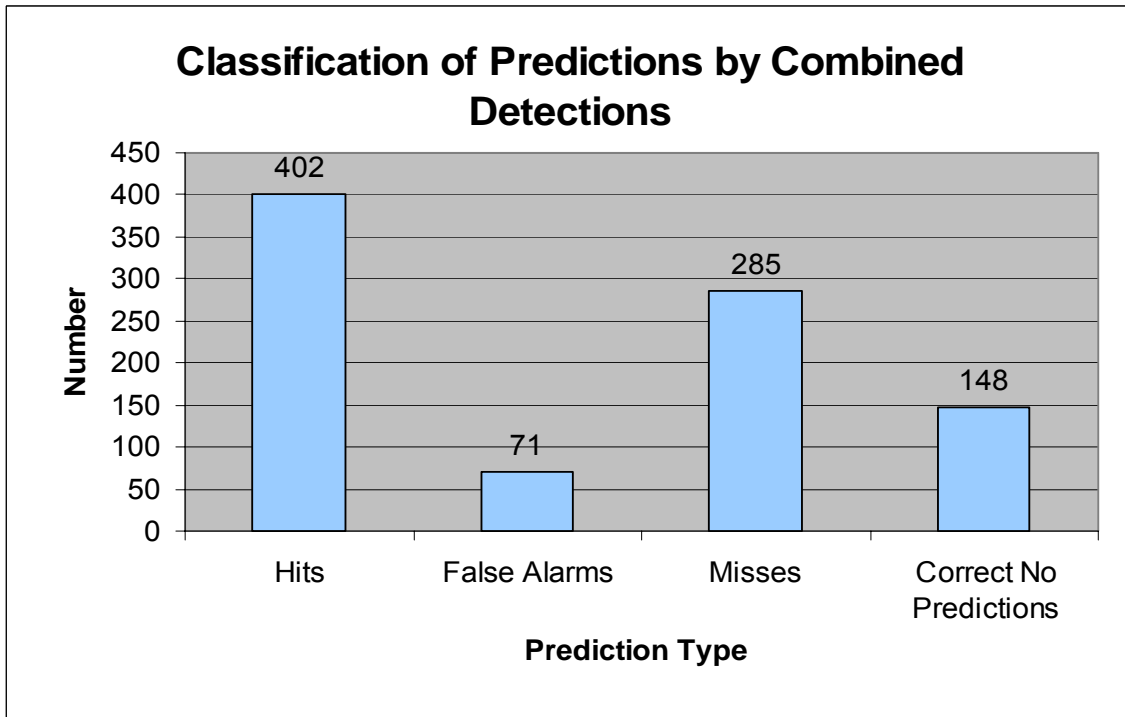


Fig. 8. Summary for severe weather predictions utilizing combined detections.

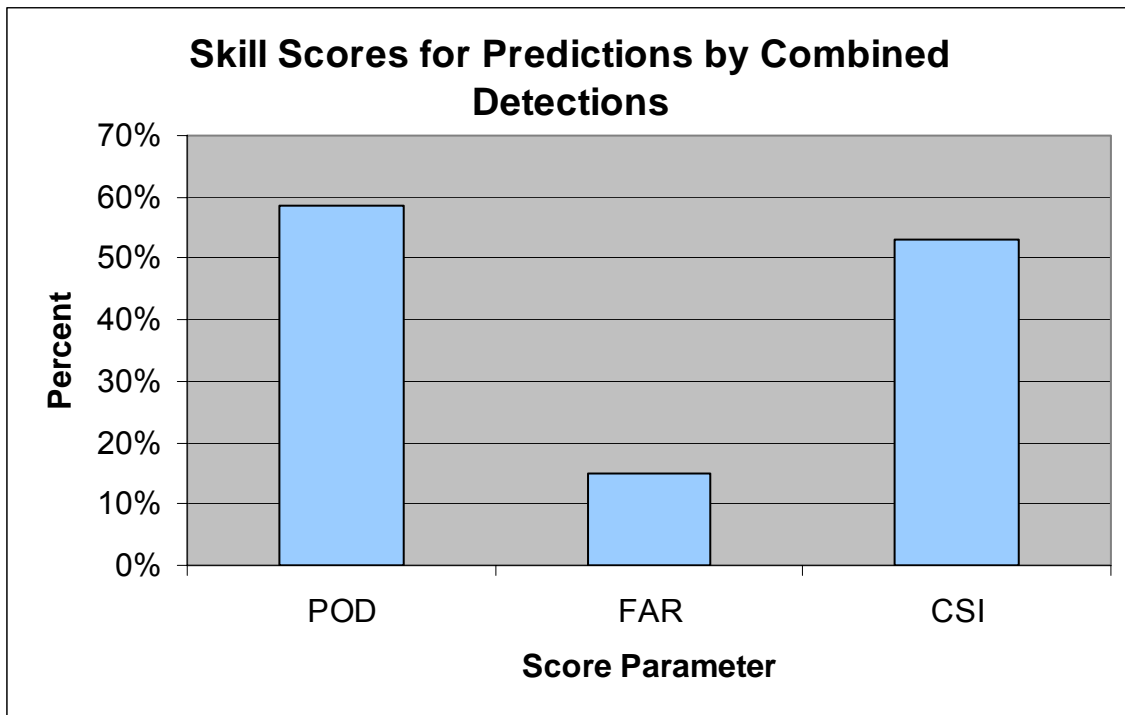


Fig. 9. Skill scores for the utilization of combined detections as predictors of severe weather. POD, FAR, and CSI are defined by Eqs. (1-3), respectively.

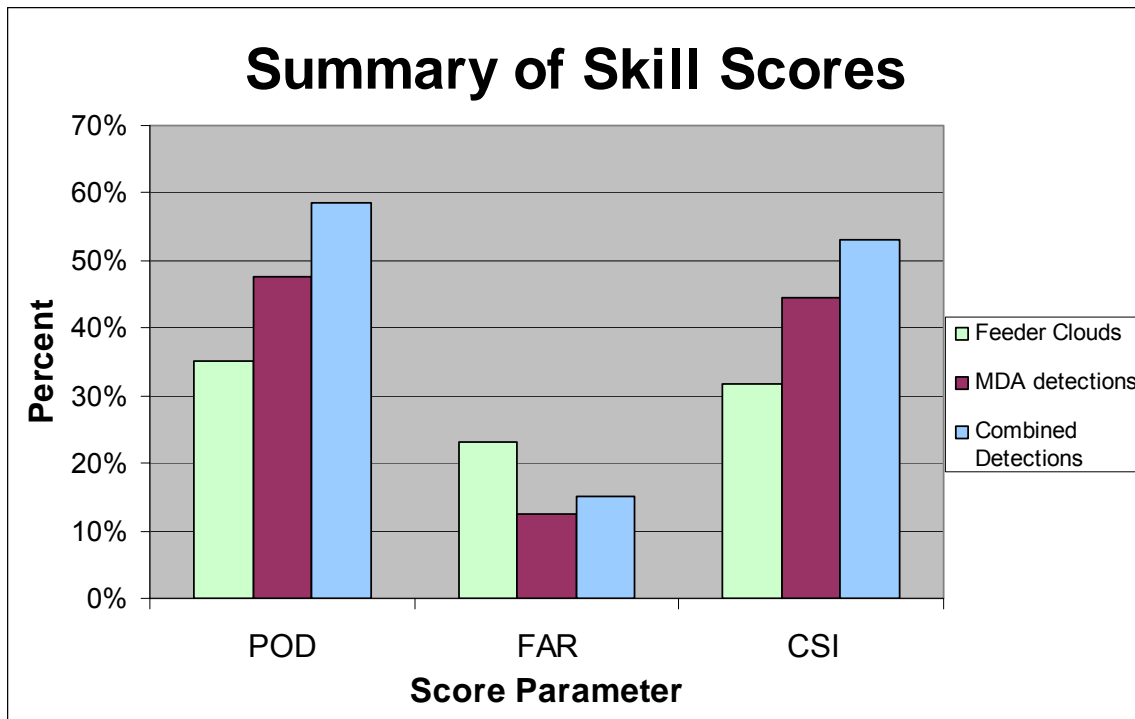


Fig. 10. Summary of skill scores for all three predictors of severe weather. POD, FAR, and CSI are defined by Eqs. (1-3), respectively.

**Table 1. Severe Weather Days, Number of Thunderstorms, and Thunderstorm Location**

<b>Date</b>	<b>Number of Storms</b>	<b>Thunderstorm Location by State</b>
22-May-96	4	Nebraska, Wyoming, and Colorado
27-May-97	6	Texas, Louisiana, and Arkansas
16-Apr-98	6	Kentucky, Tennessee, and Mississippi
2-Jun-98	8	West Virginia, Pennsylvania, and New York
13-Jun-98	2	Nebraska and Kansas
21-Jan-99	5	Alabama, Georgia, Mississippi, and Louisiana
5-Jun-99	3	Nebraska and Kansas
13-Feb-00	3	Arkansas Louisiana
18-Apr-02	5	Iowa, Illinois, and Wisconsin
7-May-02	7	Texas, Oklahoma, and Kansas
19-Apr-03	4	Oklahoma and Texas
4-May-03	16	Oklahoma, Kansas, Nebraska, and South Dakota
8-May-03	9	Kansas, Nebraska, and Oklahoma
22-Jun-03	4	Wyoming, Nebraska, Kansas, and Iowa
24-Jun-03	9	South Dakota, Minnesota, Iowa, and Kansas
20-Apr-04	2	Illinois and Iowa
10-Jun-04	8	South Dakota, Nebraska, and Kansas
4-Aug-04	4	Oregon and Idaho
7-Jun-05	5	Wyoming and South Dakota
9-Jun-05	3	Nebraska, Kansas, and Oklahoma
27-Jun-05	3	Wyoming, Colorado, Kansas, Nebraska
9-Aug-05	4	Minnesota and Wisconsin
18-Aug-05	4	Wisconsin, Illinois, and Indiana
31-May-06	6	Colorado and Wyoming

**Table 2. Severe Weather Days Analyzed Using Radar Imagery and Number of Thunderstorms**

<b>Date</b>	<b>Number of Storms</b>
27-Jun-05	3
18-Apr-02	5
7-May-02	7
8-May-03	9
7-Jun-05	5
4-Aug-04	4
19-Apr-03	4
2-Jun-98	3
16-Apr-98	6

<b>Table 3. Contingency table used to score the occurrence of feeder clouds and mesocyclone detections</b>			
		<b>Observed Event</b>	
		Yes	No
<b>Algorithm prediction</b>	Yes	a. HIT	b. FA
	No	c. MISS	d. CORRECT NO PREDICTION

<b>Table 4. Example of the method to classify visible and radar imagery scans.</b>									
<b>Storm #</b>	<b>Time of Report (UTC)</b>	<b>Time of Satellite Scan (UTC)</b>	<b>Observation of Feeder Clouds</b>	<b>Classification</b>	<b>Time of Radar Scan (UTC)</b>	<b>Mesocyclone Detection</b>	<b>Class.</b>	<b>Combined Detection</b>	<b>Class.</b>
3		2210	No	CNP	2209	No	CNP	No	CNP
		2215	Yes	FA	2213	Yes	FA	Yes	FA
					2218	Yes	FA	Yes	FA
		2225	Yes	HIT	2223	No	MISS	Yes	HIT
					2228	Yes	HIT	Yes	HIT
		2232	Yes	HIT	2233	Yes	HIT	Yes	HIT
		2240	Yes	HIT	2238	Yes	HIT	Yes	HIT
		2245	Yes	HIT	2243	No	MISS	Yes	HIT
					2248	Yes	HIT	Yes	HIT
	2250-2303	2255	Yes	HIT	2253	Yes	HIT	Yes	HIT
					2258	No	MISS	Yes	HIT
		2302	Yes	HIT	2303	Yes	HIT	Yes	HIT
	2303-2306	2310	Yes	HIT	2308	No	MISS	Yes	HIT
		2315	Yes	HIT	2313	No	MISS	Yes	HIT
					2318	No	CNP	Yes	FA
		2325	Yes	FA	2323	Yes	FA	Yes	FA
					2328	Yes	FA	Yes	FA
		2332	Yes	FA	2333	Yes	FA	Yes	FA